Accepted version; ACS Appl. Mater. Interfaces 2023, 15, 43, 50058–50068

Anti-fouling Coatings from Glassy Polyelectrolyte Complex Films

John Akintola, Yuhui Chen, Zachary A. Digby, Joseph B. Schlenoff*

Department of Chemistry and Biochemistry

The Florida State University

Tallahassee, FL 32308-4390 USA

*Email: jschlenoff@fsu.edu

Keywords: coacervate, zwitterion, algae, foul-release, multilayer, LbL, viscoelasticity, glass transition

Abstract

Coatings that prevent or decrease fouling are sought for many applications, including those that inhibit the attachment of organisms in aquatic environments. To date, antifouling coatings have mostly followed design criteria assembled over decades: surfaces should be well/strongly hydrated, possess low net charge and maintain a hydrophilic character when exposed to the location of use. Thus, polymers based on ethylene glycol or zwitterionic repeat units have been shown to be highly effective. Unfortunately, hydrated materials can be quite soft, limiting their use in some environments. In a major paradigm shift, this work describes *glassy* antifouling films made from certain complexes of positive and negative polyelectrolytes. The dense network of electrostatic interactions yields tough materials below the glass transition temperature, T_g, in normal use, while the highly ionic character of these polyelectrolyte complexes ensures strong hydration. The close proximity of equal numbers of opposite charges within these complexes mimics zwitterionic structures. Films, assembled layer-by-layer from aqueous solutions, contained sulfonated poly(ether ether ketone), SPEEK, a rigid polyelectrolyte which binds strongly to a selection of quaternary ammonium polycations. Layer-by-layer buildup of SPEEK and polycations was linear, indicating strong complexes between polyelectrolytes. Calorimetry also showed complex formation was exothermic. Surfaces coated with these films in the 100 nm thickness range completely resisted adhesion of the common flagellate green algae, *Chlamydomonas reinhardtii* which were removed from surfaces at the minimum applied flow rate of 0.8 cm s^{-1}. The total surface charge density of adsorbed cations, determined with a sensitive radioisotopic label, was very low, around 10% of a monolayer, which minimized adsorption driven by counterion release from the surface. The viscoelastic properties of the complexes, which were stable even in concentrated salt solutions, were explored using rheology of bulk samples. When fully hydrated, their T_gs were observed to be above 75 ^oC.

Introduction

In aquatic environments, surfaces are fouled by organisms from the micro- to the macro-scale under a variety of mechanisms. Fouling increases fuel consumption, decreases service life, accelerates corrosion and brings with it the possibility of introducing invasive species into aquatic ecosystems.[1, 2, 3] Both vessels and installations/infrastructure are subject to fouling. The progress of fouling includes both sequential and simultaneous elements from a broad variety of biological or bio-derived agents.

The preparation of antifouling and fouling release surfaces represents one of the most stringent challenges in materials and surface science. This is because Nature has evolved a plethora of mechanisms by which organisms may attach to surfaces – a property needed for their survival. Historically, practical antifouling or nonfouling coatings have relied heavily on toxic components to actively discourage fouling. As environmental concerns surrounding toxic coatings have increased, tin[4] has given way to copper and a variety of organic biocides[5] as active antifouling components in marine paints. Fluorinated hydrocarbons are also starting to generate environmental concerns, due to the inertness and thus “forever” qualities of some fluorinated materials, especially those used to make surfaces “nonstick.” [6]

Some currently-used antifouling coatings are designed to allow the removal of accumulated biomaterials under shear – fouling release - a property claimed by some polydimethylsiloxanes (PDMS).[7] Other coatings are designed to hydrolyze slowly promoting loss of adhesion under shear in self-polishing formulations. In the ideal passive antifouling surface, the physical and chemical characteristics of the surface are sufficient to deter adhesion under static and flow conditions. In practice, the line between antifouling and fouling release is sufficiently blurred such that a small amount of shear may be required to remove a colony of organisms adhering to a "passive" antifouling surface.

Antifouling surfaces are sought for a variety of environments, from physiological (biomedical) to environmental. Materials for passive antifouling coatings have many properties in common. They are usually neutral or weakly negative, and well hydrated: what Ikada[8] termed a "superhydrophilic diffuse surface." Ikada's criteria have guided antifouling materials development, as the properties thought to be essential for reducing nonspecific adsorption to surfaces include good hydration, (near) neutral charge, minimal disruption of water structure, and complete coverage of the underlying surface. Numerous hydrophilic, net-neutral monomers and polymers fulfill such critera,[9] including acrylamides, polysaccharides (e.g. mannitol[10]), and, most commonly, polymers or oligomers based on the ethylene glycol, EG, (-CH_2-CH_2-O-) repeat unit, termed PEGs. Superhydrophilicity in a coating implies a high water content, which is achieved with the use of polymer brushes[11, 12, 13] or thin films of hydrogels.

Zwitterions are both net-neutral and hydrophilic[14] and may be deployed as a dense monolayer (as in the cell membrane) or as repeat units in polymer layers. The antifouling properties of zwitterions were initially directed towards biomedical applications, such as preventing protein and bacterial adhesion *in vivo.*[15] Zwitterionic polymer brushes may be grafted *to*,[16, 17] or grafted *from*,[18, 19 20] surfaces. Zwitterion brushes grown from surfaces have been extensively reported by Jiang's group.[14, 21, 22] These coatings demonstrated particularly effective fouling resistance, even from pure serum. Bacterial adhesion was also inhibited.[23]

Any broadly-adopted solution to environmental fouling must be commercially scalable and rugged. Ikada's design criteria are at odds with those proposed applications where substrates are exposed to physically demanding environments. Though effective under controlled laboratory conditions, or in physiological environments,[24] a strong degree of hydration[14] means zwitterionic brushes or hydrogels are soft and lack the resilience needed to withstand practical marine environments. Brushes tend to spontaneously detach[25] since most have only one anchor point[26] yet they rely on steric/elastic forces to stretch away from the surface. Efforts to stabilize brushes have met with partial success.[27]

During our investigations into the basic science of polyelectrolyte complexes, where interactions between positive, Pol^+, and negative, Pol^-, repeat units form a dense network of physical crosslinks between polyelectrolytes, we found that they shared some key properties with polymeric zwitterions. The charges within the material may be stoichiometric and Raman scattering showed they do not disrupt the hydrogen-bonding structure of water,[28] as found in polyzwitterions.[29] In addition, PECs do not shrink in salt water. The charge pairing within PECs, and the fact that they contain no salt in pure water, suggested they could be viewed as "zwittersolids" (Scheme 1).[30]

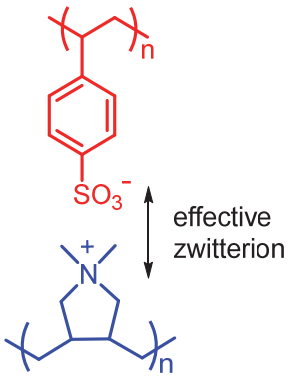

Scheme 1. Example of functional groups interacting within a PEC. Because the ratio of positive to negative groups is 1.0:1.0 and there are no ions in the solid, the combination of charges at a fixed distance mimics the zwitterion functionality.

Under the right conditions, equal number of positive and negative polyelectrolyte units combine, leaving a bulk and a surface that are substantially free of excess polymer charge or counterions. For example, the combination of poly(diallyldimethylammonium), PDADMA, and poly(styrene sulfonate), PSS, is glassy when hydrated (T_g of about 34 °C).[31] The surface charge, reflected by the number of counterions per cm^2, of a PDADMA/PSS multilayer can be less than 10% of a monolayer.[32] The effective antifouling properties of a recently-reported trimethylene N-oxide zwitterionic polymer was attributed to the proximity of the opposite charges and their stronger hydration.[33] The distance between charges in the effective zwitterion shown in Scheme 1 is also short.

Ultrathin coatings of PECs with antifouling properties have been prepared using the layer-by-layer method of assembly (polyelectrolyte multilayers, PEMUs).[34, 35, 36, 37, 38, 39, 40] Soft and well hydrated, these coatings have followed the accepted design principles. In this work, we present a new class of *glassy,* rugged coatings from complexed polyelectrolytes which proved counterintuitively effective at preventing fouling by *Chlamydomonas reinhardtii*, native to aquatic environments.[7,18] *C. reinhardtii* is an eukaryotic unicellular green microalgae possessing two flagella.[17] Commonly found growing in freshwater and soil, it is a suitable model fouling organism in freshwater aquatic environments.[41,42] The films were prepared with sulfonated poly(ether ether ketone), a widely used “engineering polymer” with a stiff hydrophobic backbone. A flow chamber[43] enabled differentiation between antifouling and foul release properties of coatings.

Experimental

Materials. Poly(ether ether ketone) (PEEK) powder, from Evonik (VESTAKEEP™ 4000 FP), or Victrex (450 PF) was dried at 120 °C for 5 h under vac. Concentrated sulfuric acid (Sigma-Aldrich, ACS grade, 96.7 wt. %) was used as received. Poly(diallyl dimethylammonium chloride) (PDADMAC, 20 wt. % in water, molar mass 400,000 – 500,000), poly(4-styrenesulfonic acid) (PSS, 18.89 wt. % in water, molar mass 75,000), and poly(vinylbenzyltrimethylammonium chloride) (PVBT, 26.9 wt. % in water, molar mass 100,000) were from Sigma-Aldrich. Methacryloylaminopropyl trimethylammonium chloride (MAPTAC, 50 wt. % solids in water) was polymerized via free radical polymerization to obtain the polymer PMAPTAC (molar mass

350,000), poly (acrylic acid) (PAA, 24 wt. % in water, molar mass 240,000) was obtained from Scientific Polymer Products Inc. and neutralized with LiOH. Lithium hydroxide (anhydrous) was from Fisher and stored in the glovebox. Sodium chloride (99.5%) was used as received from Sigma-Aldrich. Deionized water (> 18 MΩ cm) was used throughout. Silicon wafers (Si 100, double-side-polished, DSP, Prime grade, 0.5 mm thick) were from Okmetic and broken into ca. 2 cm x 2 cm pieces.

Chlamydomonas reinhardtii (+) (Carolina Biological) was cultured as described by Sager and Granick.[44] Cultures were grown in a 14 h light/10 h dark cycle at 25 °C to a density of 5 x 10^6 cells mL^{-1} as determined using a hemocytometer (Neubauer). A parallel plate flow chamber channel (75 mm long x 25 mm wide x 1 mm high) built in-house was used to study the influence of flow rate on algae detachment from PEMUs coated on glass microscope slides. Bare microscope slides were used as a control. Microscope slides were pre-cleaned with ethanol then flamed before multilayers were deposited onto the substrate using the layer-by-layer method.[45] The PEMU coated substrate was then immediately dipped into a solution containing the algae for 24 h with stirring, after which it was removed gently and placed in the flow chamber**.** Images were collected using the Nikon Eclipse TS100 microscope fitted with a Nikon DS-Ri1 Camera.

PEEK Sulfonation. Sulfonation of PEEK was carried out by adding 10 g of dry PEEK powder to 100 mL sulfuric acid. The mixture was stirred in a three-necked flask at 75 ± 1 °C for 6 h under N_2.[46] Following sulfonation, the dissolved sulfonated PEEK, SPEEKH, was precipitated by pouring it into 500 mL ice cold water. The precipitated sample was repeatedly washed on a vacuum filter with ice cold water to remove excess sulfuric acid. The washed sample was then re-heated at 50 °C in small amount of deionized water to dissolve the SPEEKH. The SPEEKH was neutralized with 1 M LiOH (Scheme 1). Neutralized SPEEK (SPEEKLi) was dialyzed against water for two weeks with water replacement twice a day. Solid SPEEKLi was then obtained by freeze drying the product.

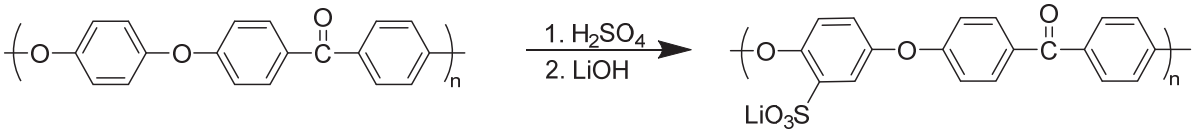

Scheme 2. Sulfonation of PEEK

Hydrodynamic Radius. Dynamic light scattering was used to measure the SPEEK hydrodynamic radius, R_h, with a goniometer system (ALV/LSE-5004) equipped with a He-Ne laser (λ = 632 nm, 22 mW) at a 90° collection angle. Measurements were taken in 10 mm capped cylindrical borosilicate glass tubes through a reservoir containing a refractive index matching liquid (toluene). The samples were 1 mg mL^{-1} in aqueous 0.3 M LiCl, filtered through a 0.1 μm Millipore filter. The R_h was calculated along with the distribution of R_h by pseudo-cross-correlation of the signals obtained by the two photomultipliers. The intensity autocorrelation function $g^{(2)}(q,\tau)$ where $q = 4\pi n_D \sin(\Theta/2)/\lambda$ was obtained with suppressed noise by using ALV correlator software V.3.0.

Layer by Layer Buildup. Multilayers from PMAPTA/SPEEK, PDADMA/SPEEK, PVBT/SPEEK, PVBT/PSS, PDADMA/PSS and PDADMA/PAA were built using a robot (StratoSequence V, nanoStrata Inc.) on DSP silicon wafers, which allowed transmission FTIR, or on single-side-

polished Si wafers for ellipsometry and AFM measurements. PEMUs were also built on clean fused silica slides for UV-vis absorbance measurements. All substrates were cleaned in "piranha" (70 % H_2SO_4/30 % H_2O_2) for 30 min after which they were vigorously rinsed with water and dried with a stream of N_2. (Caution! Piranha is strongly oxidizing and should not be stored in closed containers.). Polymers solutions were 10 mM (based on the repeat unit) for ellipsometry, transmission FTIR and algae adhesion measurements. The substrates were mounted onto a shaft and rotated at 300 rpm. Substrates were alternately dipped in each polymer for 10 min, starting with the polycation, followed by three 1 min rinsing steps in water. Multilayers with an odd number of layers (terminating in polycation) have a positive surface charge whereas even numbers of layers yielded negative surfaces.

Streaming Potential Measurement. Surface streaming measurements were obtained using an in-house built electrokinetic flow cell with a parallel plate configuration (see Supporting Information Figure S1). A clean microscope slide (75 mm x 25 mm) was inserted on the bottom half of the cell while the top glass had 1 mm holes allowing inlet and outlet flow of electrolyte. The top and bottom glass slides were clamped together using a rubber spacer (length = 17 mm, width 5 mm and height of 0.1 mm) creating a micro-flow channel. The parallel plate set-up (at the glass-liquid interface) were fitted with silver wire electrodes connected to a Keithley voltmeter to measure the streaming potential. A 10 L reservoir with a pressure gauge containing 1 mM NaCl was pressurized with N_2 to force electrolyte through the cell. The pressure difference across the sensor wires was measured with a calibrated Validyne P55 differential pressure transducer. The zeta potential, ζ (mV), was calculated using the following equation:[47]

$$\frac{E_S}{\Delta P} = \frac{\varepsilon_r \varepsilon_o \zeta}{\lambda_b \mu} \qquad [1]$$

where E_s is the measured streaming potential (mV). ΔP, the pressure drop between the Ag sensor electrodes, was 1.87×10^4 Nm^{-2}. μ, the viscosity of the streaming solution was, 1.0×10^{-3} Nsm^{-2}, ε_r, the relative dielectric permittivity of the streaming solution was 80 while ε_0 is the permittivity of vacuum, 8.85×10^{-12} Ssm^{-1}. Bulk solution conductivity, λ_b was 2.19×10^{-2} Sm^{-1} as measured using an Orion 3 Star 4-point conductivity probe and meter from Thermo Scientific.

Surface Charge Radiolabeling. The actual number of $SPEEK^-$ charges on SPEEK-terminated surfaces was measured using ultrasensitive radiolabel techniques. Si wafers approximately 2 cm x 2 cm coated with 10 layers (terminating in SPEEK) were used. Wafers were exposed on one side to 300 μL 2.5 x 10^{-5} M ^{14}C-labeled tetraethylammonium bromide (^{14}C-TEABr from Perkin Elmer Radiochemicals, specific activity 3.5 Ci mol^{-1}) for 1 h. We have shown previously that the TEA^+ cation only labels the surface negative sites on multilayers.[32] The solution was blown off the surface with a jet of N_2. The labeled TEA on the surface was extracted with 300 μL of 1 x 10^{-3} M unlabeled TEABr. This 300 μl was mixed with 2 mL of water-tolerant liquid scintillation cocktail (Ecolite, MP Biochemicals) and counted in a Charm II counter (Charm Sciences). 300 μL of 2.5 x 10^{-5} M ^{14}C-TEABr was used as a standard to convert counts per minute, cpm, to moles of ions per cm^2. Wafers coated with 3 layers (PDADMA/SPEEK/PDADMA), to which TEA^+ does not adsorb, were used as background, employing the same procedure as with the SPEEK-terminated multilayers. Typical counts on the SPEEK surfaces were around 400 cpm, and those on the background were about 70 cpm, which were from the film of electrolyte that remained after jet-blowing the surface.

Ellipsometry The dry thicknesses of PEMUs prepared on Si wafer were obtained by using a Gaertner Scientific L116S autogain variable-angle Stokes ellipsometer equipped with a He-Ne laser (632.8 nm) at an incident angle of 70^{o}, fixing the refractive index of the films at 1.54 and that of Si (substrate) at 3.85. Ten thickness measurements on each PEMU were averaged. A native oxide layer of about 1 nm was subtracted from the measurements.

NMR Characterization. ^{1}H solution NMR spectroscopy (Bruker Avance 400 MHz) was used to determine the degree of sulfonation.[48] Dry SPEEKLi (sulfonated from Vestakeep^{TM} 4000 FP PEEK)**,** was dissolved in a 90:10 DMSO:D_2SO_4 solvent mixture ratio while dry SPEEKLi (sulfonated from Victrex 450 PF PEEK), was dissolved in a 95:5 DMSO:D_2SO_4 mixture to obtain 15 mg mL^{-1} solutions.

FTIR Studies. Transmission Fourier transform infrared (FTIR) spectra of samples prepared on DSP Si wafers were obtained with a Nicolet Nexus 470 FTIR spectrometer with a DTGS detector. The resolution was 4 cm^{-1}, and 256 scans were averaged for each sample. Samples were held at 15^{o} off-perpendicular to reduce any interference fringes. The background for all spectra was taken on uncoated Si. Attenuated total reflection – Fourier transform infrared (ATR-FTIR) spectra were collected using a ThermoScientific Nicolet is20 equipped with a Pike MIRacle ATR attachment fitted with a single-reflection diamond/ZnSe crystal and a high-pressure clamp. Here, background for all spectra was ambient air.

UV-Visible Spectroscopy (UV-vis). UV-vis spectra were collected with a Cary 100 Bio UV-Vis spectrometer. UV-vis spectra were recorded on 0.05 mM SPEEKLi in 0.3 M LiCl and on multilayers on fused silica slides.

Contact Angle Measurements. Water contact angles on PEMUs were measured using a contact angle goniometer (KSV Instruments, CAM 200) at room temperature. The static contact angle was digitally captured using a 70μL mL water droplet, and image analysis software was used to measure the contact angles.

Atomic Force Microscopy Images. Images of the surface of PEMUs were recorded with a Dimension Icon Scanning Probe Microscope (SPM), equipped with a NanoScope V controller and NanoScope software (in tapping mode), and silicon OTESPA probes (Bruker, 0.01 - 0.02 Ω cm Si, tip radius = 7 ± 2 nm, cantilever thickness = 4.6 μm, length = 160 μm, width = 50 μm, resonance frequency 300 kHz, spring constant k = 42 N m^{-1} coated with Al). Images were scanned at a rate of 1 Hz, with a scan size of 5 μm x 5 μm. The rms roughness was measured on 5 different 1 μm x 1 μm scan areas and averaged.

Stability of Films. The stability of the three SPEEK multilayers in salt was tested by exposing them to 2 M NaCl and 3 M NaCl for 1 week at room temperature. Thicknesses of 10-layer multilayers on Si wafer were measured using ellipsometry before and after exposure. Scanning Electron Microscopy, SEM, images of films were also acquired before and after salt exposure using a JEOL JSM-IT800 field emission SEM equipped with a secondary electron detector (SED) at 5 kV accelerating voltage. Samples were rinsed in water before imaging to remove salt. Some of the multilayers were scratched with tweezers to reveal the film profile.

Rheology of Polyelectrolyte Complexes, PECs. Complexes for bulk rheology were prepared by simultaneously combining stoichiometric mixtures of 10 mM polyelectrolyte solutions in 0.3 M LiCl. The PECs were annealed at 60 ^{o}C for 7 h to ensure 1:1 good mixing. Precipitates were equilibrated in 0.01 mM LiCl followed by water to remove any excess salt. Tablets (8 mm diameter x 2 mm thickness) of PDADMA/SPEEK, PVBT/SPEEK and PMAPTA/SPEEK PECs were prepared by wet compression molding with 0.01 M LiCl electrolyte using a steel mold at temperatures close to the glass transition temperature, $T_{g,}$ of the complex. Using a stress-controlled DHR-3 rheometer (TA Instruments), the linear viscoelastic response, LVR, of the complexes was investigated as a function of temperature. The tablets were placed on the lower plate of the rheometer and compressed using 1 N axial force. During rheology, all samples were maintained in a reservoir containing 0.01 M LiCl so that they would remain fully hydrated. After use, tablets were weighed, dried at 120 ^{0}C to constant weight, and weighed again to determine the water content.

Isothermal Titration Calorimetry (ITC). Isothermal calorimetry was performed using a VP-ITC (MicroCal Inc.) calorimeter. The ITC was calibrated with an internal y-axis calibration followed by a standard titration between hydrochloric acid and Tris base. All samples were degassed for 10 min at room temperature. Approximately 300 µL of 10.0 mM polycation in 0.30 M LiCl was loaded into the syringe. Ten microliters of the solution was manually discharged from the syringe to relieve any back pressure from the loading process. The sample cell (1.4138 mL) was washed, then loaded, with 0.5 mM SPEEKLi in 0.30 M LiCl. Prior to injection, the ITC was allowed to equilibrate at 65.0 °C. The syringe was rotated at 260 rpm in the sample cell with an injection size of 4 µL per aliquot at a rate of 0.50 µL s^{-1}, with 240 s between injections. The heat flow was recorded as a function of time at 65.0 °C for all samples. Enthalpies were calculated by summing the total heat generated to the 1:1 end point with a correction for the background dilution enthalpy.

Results and Discussion

Whether polyelectrolyte complexes in general are glassy or liquid-like is not reliably correlated to the water content.[31] Water plasticizes PECs to a point,[49, 50] after which it appears to simply dilute the dense crosslinks inherent to complexes. The chemical identity of the charge pairing interactions is important, as some combinations of Pol^{+} and Pol^{-} provide slower pairing dynamics. Most of the polyelectrolyte pairs used here produce glassy material when combined as a complex, even when they are fully hydrated in salty water.[31] Though previously employed in PEMUs,[51] the potential glassy nature of PECs containing sulfonated PEEK has not been established. SPEEK is rod-like with high aromatic content and a charge of one sulfonate per three aromatic rings (see Scheme 2). SPEEK was prepared by sulfonation of PEEK using concentrated H_2SO_4 at 75 ^{0}C. The ^{1}H NMR spectrum showed full sulfonation according to the structure in Scheme 2 (see Supporting Information Figure S2) without evidence of additional charge. The FTIR spectra are also consistent with full sulfonation (Supporting Information Figure S3).

A versatile method to produce ultrathin films of PEC employs the layer-by-layer assembly of component polyelectrolytes (see Scheme 3) from aqueous solution.[45] The layers may be produced by alternating dipping or, much more quickly, by alternating spraying of individual

polyelectrolytes[52] usually starting with the polycation, as ambient surfaces are commonly negatively charged. Various combinations of polycations and polyanions assembled as multilayers have been reported to reduce fouling. Kurtz et al.[53] reported that when compared to control glass slides, PDADMA/PSS films reduced the adhesion of *E. coli*. Zhu et al.[54] reported that layer-by-layer films (crosslinked and non-crosslinked) demonstrated antifouling properties by preventing the adhesion/settlement of amphora and cyprids under static experimental conditions. We have previously reported that a coating of PSS on DOWEX X8 anion-exchange resin prevented fouling by *C. reinhardtii*. Uncoated resins, which are positively charged, permitted significant cell attachment, sequestering about 80% of the added algae.[37]

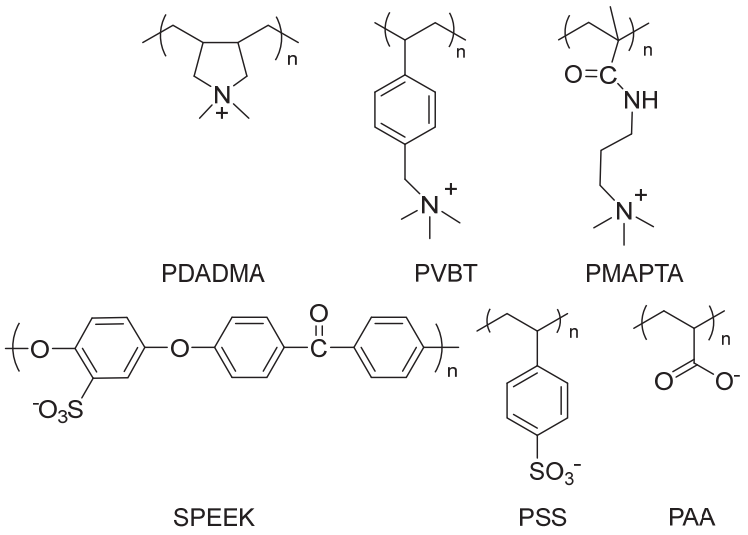

Scheme 3. Structures of polyelectrolytes employed. Counterions not shown.

Figure 1 shows a linear buildup of thickness with the number of layers deposited. Multilayer buildup was tracked using ellipsometry on the native oxide surface of silicon wafers or on fused silica via UV-vis absorption spectroscopy. Each layer was deposited from a 10 mM solution of polymer in 0.3 M LiCl by dipping in the solution for 10 mins followed by three 1 min rinses in water.

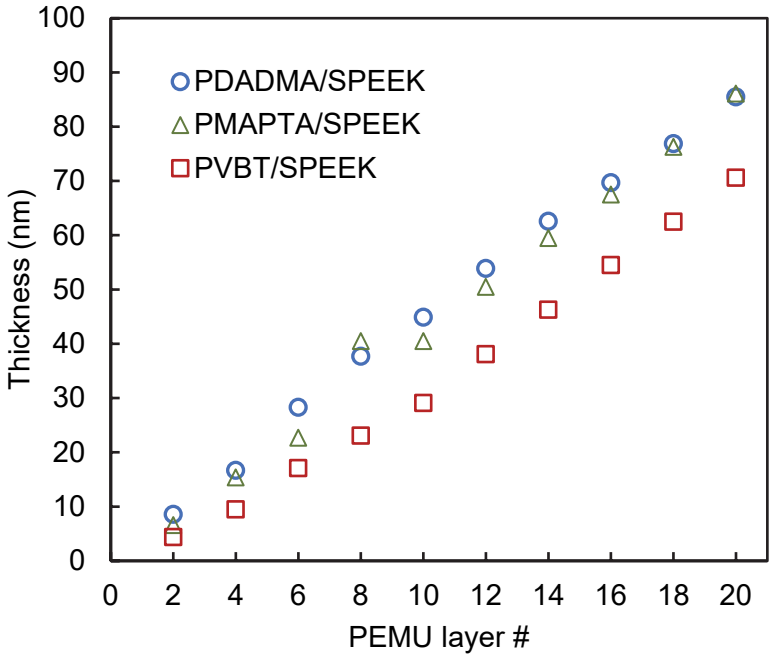

Figure 1. Film thickness as a function of the number of deposited layers for PEMUs. PDADMA/SPEEK (●); PMAPTA/SPEEK (Δ): and PVBT/SPEEK (□) deposited from 0.3 M LiCl at room temperature. All three systems grow linearly. Error bars are about the size of the data points,

Linear multilayer growth is correlated with strongly-interacting polyelectrolytes and glassy PECs in particular.[55] In such a scenario, incoming polyelectrolyte charge compensates the existing charge but does not strongly overcompensate or diffuse in,[32] meaning a small amount of polyelectrolyte is added on each "layer" and the bulk of the multilayer remains charge balanced. The liquid-like properties of weak multilayers[56] permit equilibrium excess charge, or overcompensation, to accumulate in the film, which yields nonlinear or "exponential" growth.[57] Many glassy multilayers exhibit a few layers of initial nonlinear growth (e.g. see the buildup of PVBT/PSS, T_g ~ 90 ^{0}C, in Supporting Information Figure S4). PDADMA/PSS, with a T_g of about 35 ^{0}C, transitions from nonlinear to linear after about 14 layers.[32] The immediate linearity of the SPEEK combinations is taken as an indication of strongly glassy properties. The charge density of SPEEK is low relative to many polyelectrolytes, while the backbone is relatively stiff. Sulfonation of PEEK beyond the level shown in Scheme 3 is difficult to achieve without degradation, since the introduction of the SO_3^- group in the location shown in Scheme 3 deactivates further sulfonation.[58]

While counterion release from polyelectrolytes is always present as a driving force for complexation,[28] enthalpy changes modify the strength of interactions.[56] PECs with an exothermic complexation enthalpy, ΔH_{PEC}, suggest strong complexation. Isothermal titration calorimetry, often used to measure ΔH_{PEC},[56, 59] provided surprisingly low values at room temperature. Due to the glassy nature of the complex, it was suspected that charge pairing between positive and negative repeat units was kinetically arrested and thus incomplete. When the ITC was repeated at 65 ^{o}C to accelerate this pairing, all polyelectrolytes showed exothermic complexation (see Supporting Information Figure S5). Observations of the thickness increment for each layer (see

Figure S6 for an example) showed that each SPEEK layer was about 1 nm thicker than the polycation layer, which is to be expected, since the SPEEK repeat unit is heavier than those of the Pol^+ repeat units. While this suggests good pairing between bulk Pol^+ and Pol^-, the error for each layer thickness was about ± 25%. Near-stoichiometric pairing was inferred from FTIR observations. FTIR spectroscopy of multilayers on Si wafers showed the presence of both polymers. The bands from PVBT were weak compared to those from PSS, but a spectrum of bulk complex known to be stoichiometric showed a spectrum that was almost identical to that of the multilayer (see Supporting Information Figure S7 for an example).

The surface charge switches between negative and positive depending on the identity of the last-added "layer," as seen in Figure 2. Generally, a neutral or net negative, weak surface charge favors antifouling properties.[8, 30] At the molecular level, the release of surface counterions is a strong driving force for nonspecific adsorption.[30] Therefore, surfaces with few or no charges are desired, a criterion met by PEG, polyacrylamide and other neutral hydrophilic polymers. Zwitterionic surfaces are also nominally net-neutral, though they usually bear an apparent negative charge in use.[60, 61, 62]

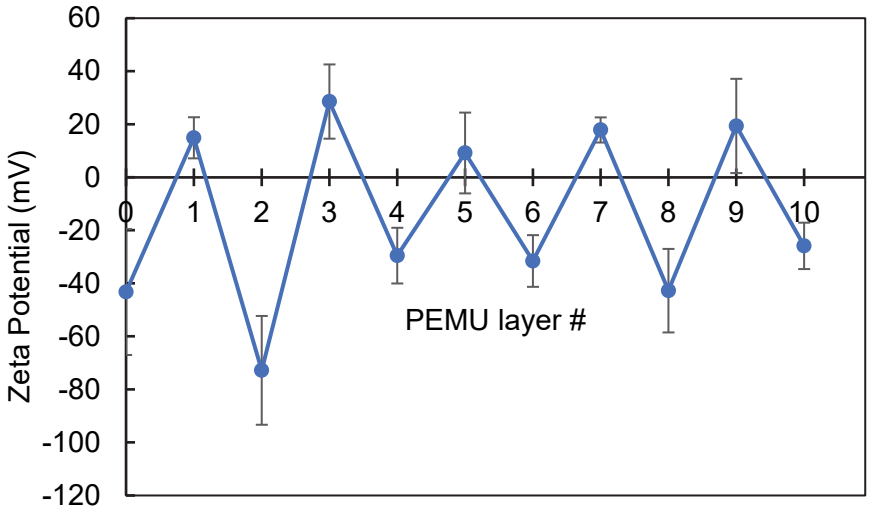

Figure 2. Zeta potential measurements during the layer-by-layer buildup of PDADMA/SPEEK in 0.3 M NaCl at room temperature. Each data point represents an average of 3 measurements under 3.5 mL s^{-1} flow using 1 mM NaCl as streaming electrolyte.

Many of the excess ions in an electrical double layer are adsorbed in the Stern layer.[63] Converting zeta potential to "apparent" surface charge does not account for these ions, which are liberated when they are exchanged by the adsorption of materials with the same charge. This ion release represents an entropic driving force.[30] The radiolabeling technique described above replaces all excess counterions at the surface, including those in the Stern layer. The ^{14}C-radiolabeled probe ion, tetraethylammonium, revealed a low population of positive counterions at SPEEK-terminated surfaces (see Table 1), consistent with a low negative charge density from

excess SPEEK. This low charge density is critical in minimizing the entropic driving force for adsorption of released counterions.

Table 1. Surface charge densities of cation (counterions) on SPEEK-terminated PEMUs

Multilayer	Molar Mass Pol^+Pol^- Repeat Unit g mol^{-1}	Surface Cation Charge Density (mole cm^{-2})	Surface Density of Pol^+Pol^- Pair[a] (mole cm^{-2})	% Monolayer of Cation Charges
PDADMA/SPEEK	531	1.60×10^{-11}	2.04×10^{-10}	7.8 ± 0.6
PVBT/SPEEK	602	1.79×10^{-11}	1.87×10^{-10}	9.6 ± 0.8
PMAPTA/SPEEK	583	3.23×10^{-11}	1.91×10^{-10}	16.9 ± 1

[a]assumes a density of PEC = 1.2 g cm^{-3}

Antifouling coatings usually benefit from a smooth surface,[64, 65] although some topographical features discourage settlement of organisms under flow.[66, 67] The surface roughness of the PEMUs was investigated using atomic force microscopy (AFM). The samples for this measurement were prepared on a single-side-polished silicon wafer. AFM images (Figure 3) showed that PDADMA/SPEEK had the lowest rms surface roughness, R_a, of 3.0 nm, followed by PVBT/SPEEK, R_a of 4.1 nm, and PMAPTA/SPEEK, with an R_a of 4.5 nm. The images reveal a few scattered features from 10-100 nm in size. Although the solution was passed through filters of (nominal) 100 nm pore size, particles smaller than 100 nm would not have been excluded. In addition, SPEEKLi is only barely soluble in water. Supporting Information Figure S8 shows dynamic light scattering results of SPEEKLi in 0.3 M and 0.5 M LiCl, with hydrodynamic radii of about 3 and 8 nm, respectively, and a tail down to 30 nm. Partial aggregation could explain the AFM features greater than 10 nm. Nevertheless, the results below suggest these features do not compromise the antifouling properties of the modified surface. Point theory[68] is commonly used to relate the interaction of micro-organisms on rough surfaces. For example, Cui et al. showed experimentally that attachment of foulants is significantly improved when the engineered surface feature was similar to the diameter of the adhering cell (foulant).[69] For our surfaces, sectional analysis (Supporting Information Figure S9) revealed roughness in orders of nanometers, significantly smaller than the model foulant *Chlamydomonas reinhardtii* which is on the order of 10 μm in size. Static water contact angles were between 43 and 72 degrees (see Supporting Information Figure S10), which are intermediate between hydrophilic and hydrophobic.

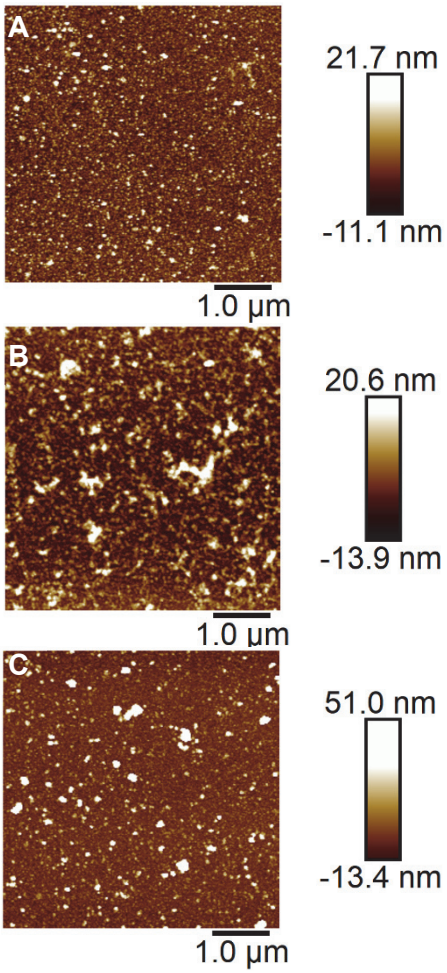

Figure 3. Atomic force microscopy images of 10-bilayer PEMUs on Si wafer showing surface topology and roughness. **A**, PDADMA/SPEEK with surface roughness, R_a, of 3.0 nm. **B**, PMAPTA/SPEEK, R_a = 4.5 nm. **C**, PVBT/SPEEK, R_a = 4.1 nm.

SEM images of 10-layer versions of the three PEMUs (45 nm thick) in Figure 3, shown in Supporting Information Figure S11, reveal the same morphology: a pinhole-free, uniform coating. Scratched areas show the smooth Si wafer underneath and fully dense films with the thickness measured via ellipsometry. Films remained adhered to the substrate when adhesive tape was pulled off them (the peel test). The stability of films in solutions of high salt concentrations was determined by measuring changes in ellipsometric film thickness after 1 week in 2 M and 3 M NaCl. Working with 10-layer PEMUs there was no significant change in the thickness (+/- 10 %) of any of the SPEEK-containing multilayers after 1 week of immersion in 2 M NaCl at room temperature. The coatings also remained intact in 3 M NaCl for a week, but appeared to become somewhat rougher (see Figure S11), perhaps a result of modest doping/swelling by the high [NaCl].

Measuring the viscoelastic properties of film of thickness < 100 nm is challenging. In contrast, there are more accurate/reliable methods of viscoelastic measurements on bulk samples. Using a rheometer, dynamic mechanical thermal analysis on stoichiometric SPEEK complexes (Figure 4) revealed that these systems were glassy with T_g of > 100 ^oC for PVBT/SPEEK, an estimated T_g of 103 ^oC for PDADMA/SPEEK, and 79 ^oC for PMAPTA/SPEEK. Storage modulus G′ remains constant at about 10 MPa, and loss modulus G″ about an order of magnitude lower, across a wide temperature range. A maximum in tanδ (= G″/G′) showing a clear T_g is only observed with PMAPTA/SPEEK (Figure 4). The water content, measured by drying the 8 mm diameter tablets after rheology was completed, is given in the caption of Figure 4.

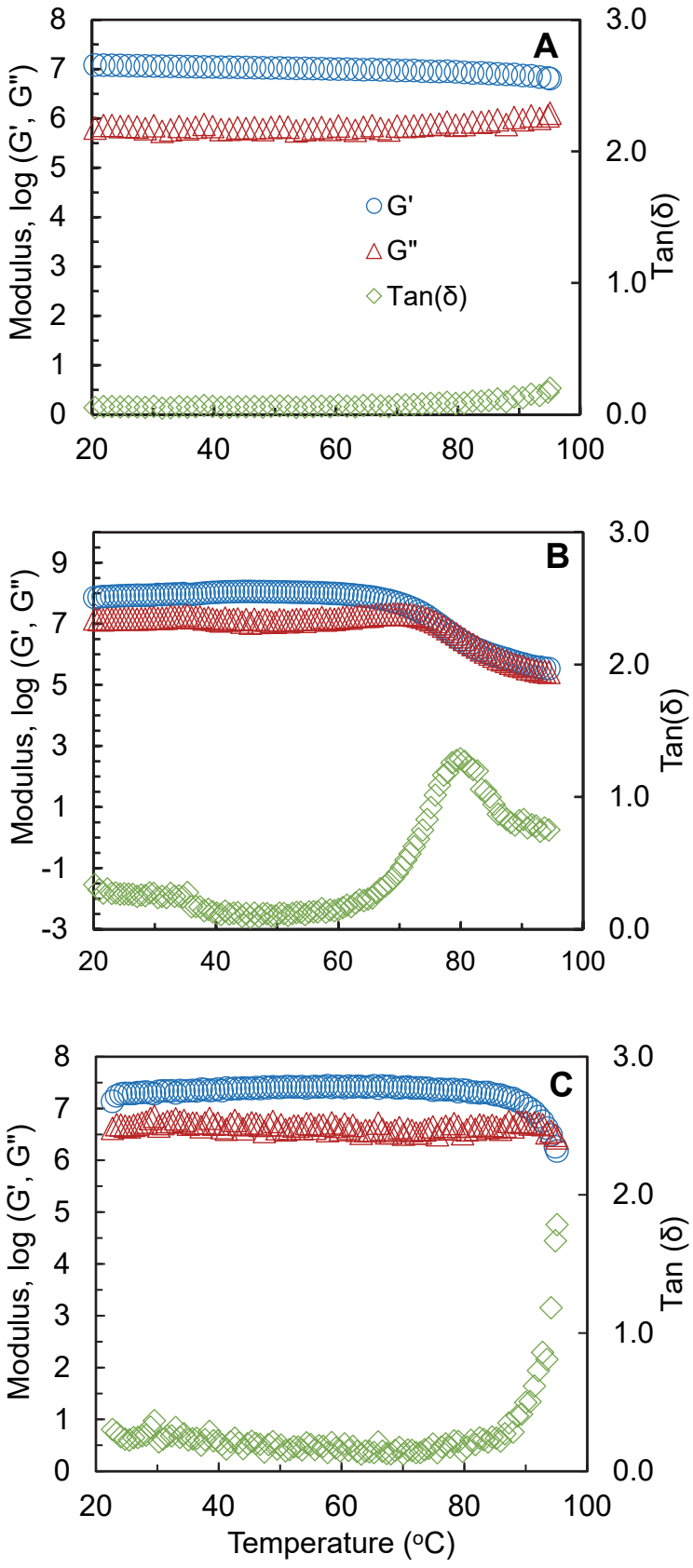
A
B
C
G'
G"
Tan(δ)
Modulus, log (G', G")
Tan(δ)
Tan (δ)
Temperature (°C)

Figure 4. Linear viscoelastic response of SPEEK complexes. Storage modulus G′ (○), loss modulus G″ (Δ) in Pa; and tan δ (◇) for **A**), PVBT/SPEEK (35 wt% water); **B**), PMAPTA/SPEEK (25 wt% water); **C**), PDADMA/SPEEK (14 wt% water) during a cooling ramp while immersed in 0.01 M LiCl. 8 mm diameter tablets. 1 N axial strain was applied at a frequency of 0.1 Hz and a ramp rate of 2 ^{o}C min^{-1}

Cell Adhesion Analysis

While passive antifouling is the ultimate property sought from these coatings, it is difficult to measure the difference between non-adhered and weakly adhered organisms or protein, as a rinsing step is usually required. In the present case, slides were maintained vertically for 24 h in a dense solution of algae under stirring, then removed carefully without rinsing and placed horizontally in a flow chamber for observation (see Supporting Information Figure S12). The same medium used to grow the algae was then passed through the chamber. The term “antifouling” in the present case refers to the population of algae removed at the lowest flow rate available (0.8 cm s^{-1} linear velocity). This is considerably less than using a “gentle stream” of media from a quirt bottle, which is a typical method of removing unabsorbed species.

Observations on 10-layer PDADMA/SPEEK multilayers, ca. 40 nm thick, showed complete removal of all algae at the minimum flow rate (Figure 5). The control, clean bare glass, showed almost no removal of algae under the same conditions.

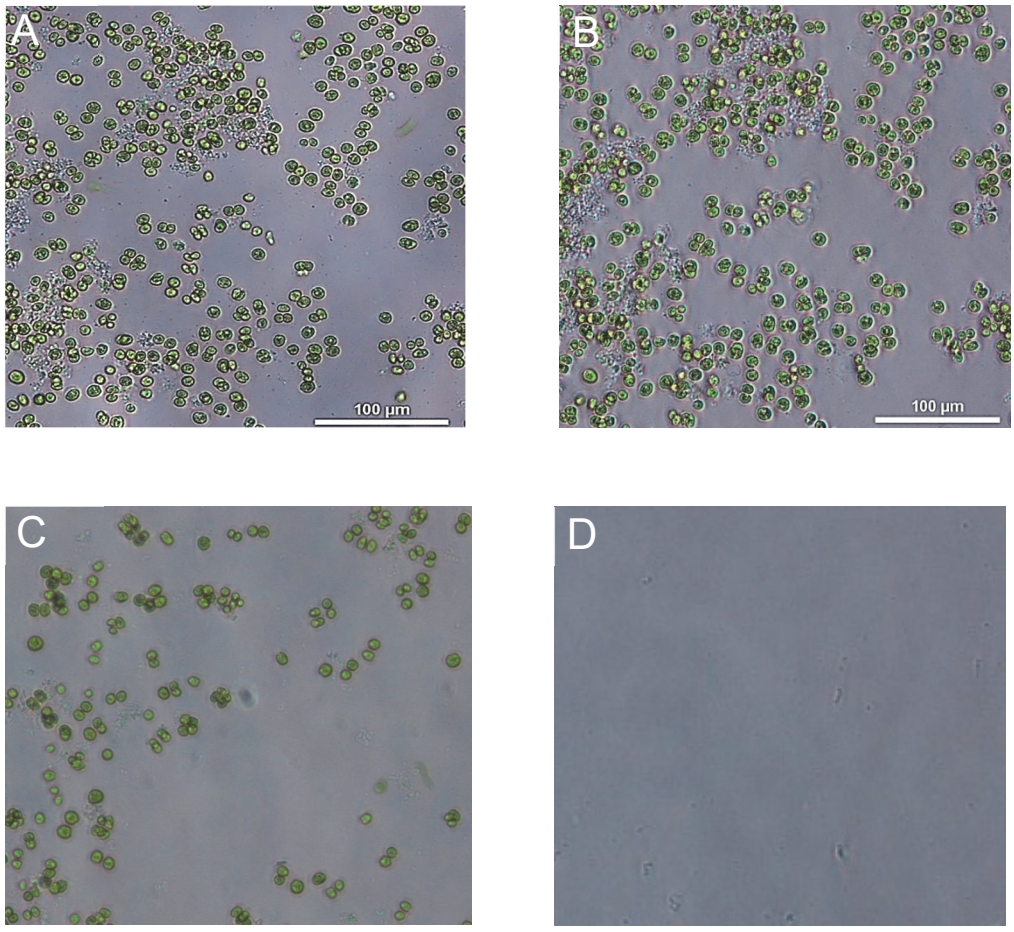

Figure 5. In-situ optical microscopy images of algae on bare glass, (**A**) before, (**B**) after flow, revealing persistent fouling; and on glass coated with 10 layers PDADMA/SPEEK of thickness ~40 nm, C) before, and (D) after the minimum applied flow rate (0.8 cm s^{-1}) showing complete detachment of algae at room temperature. Scale bar is 100 µm.

Algae attachment versus shear rate for other SPEEK-containing multilayers was compared: PMAPTA/SPEEK; PVBT/SPEEK; and also PVBTA/PSS (see Figure 6). Above a very gentle flow of 1.6 cm s^{-1} the algae were removed from most of the coatings. The as-made PMAPTA/SPEEK film showed evidence of fouling, as few cells were released to the highest flow rate employed (25 cm s^{-1}) - behavior similar to the uncoated glass control (Figure 6).

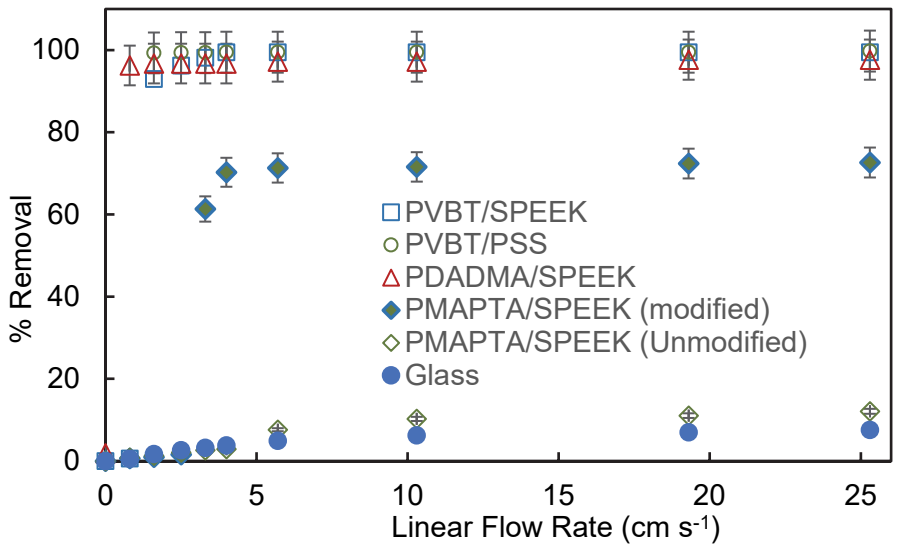

Figure 6. Profile of algae detachment under increasing flow rate at room temperature from uncoated glass (control) **(●)**; PMAPTA/SPEEK (unmodified) (◊); PMAPTA/SPEEK (modified) (♦); PDADMA/SPEEK (Δ); PVBT/PSS (○); PVBT/SPEEK (□).

Because of the poor performance of the as-made PMAPTA/SPEEK coating (Figure 6), the deposition for this pair of polyelectrolytes was modified by leaving the multilayer in the final SPEEK dip for 1 h instead of the usual 10 min. This additional contact time with the SPEEK solution allowed the accumulation of more SPEEK at the surface. As seen in Figure 6, this coating exhibited a partial fouling release response, with a minimum flow rate of 3.3 cm s^{-1} required to release about 70% of the algae. Additional algae were not released at higher flow rates. Montero et al. reported decreased biofilm formation on sulfonated PEEK surfaces.[48] The reasons the PMAPTA/SPEEK coatings were not as effective as the other two quaternary ammonium/SPEEK combinations are not known, but PMAPTA/SPEEK did have the lowest T_g (Figure 4).

A multilayer of PDADMA and PAA was used to compare the performance of a soft film. Complexes with PAA or poly(methacrylic acid) tend to have T_gs below room temperature,[31] reflected in a liquid-like or "coacervate" morphology. PDADMA/PAA is gel-like and grows exponentially in solutions containing salt. [68] A 10-layer PDADMA/PAA multilayer showed weak attachment of algae (Supporting Information Figure S13) which were mostly removed by a gentle flow of 1.6 cm s^{-1} (Supporting Information Figure S14). Increasing the flow to 20 cm s^{-1} removed the rest of the algae. However, PDADMA/PAA is not stable in salt solutions of the concentration in seawater.[70, 71] PAA combined with PAH is more tolerant of salt.[72] By encouraging a high level of hydration (and softness) in a PEMU of PAH and PAA Mendelsohn et al. showed that fibroblast adsorption was prevented.[40]

Figure 7. Summary of the population of algae adhered to PEMUs on glass terminated with, (**A**, polyanions, and panel **B**, polycations) shown here as density before and after 14 cm s^{-1} flow and percentage removal. Data with ~ 100 % removal was obtained in under 3 s while others were reported after 20 h under similar flow conditions. Data was averaged from 10 repeated individual experiments.

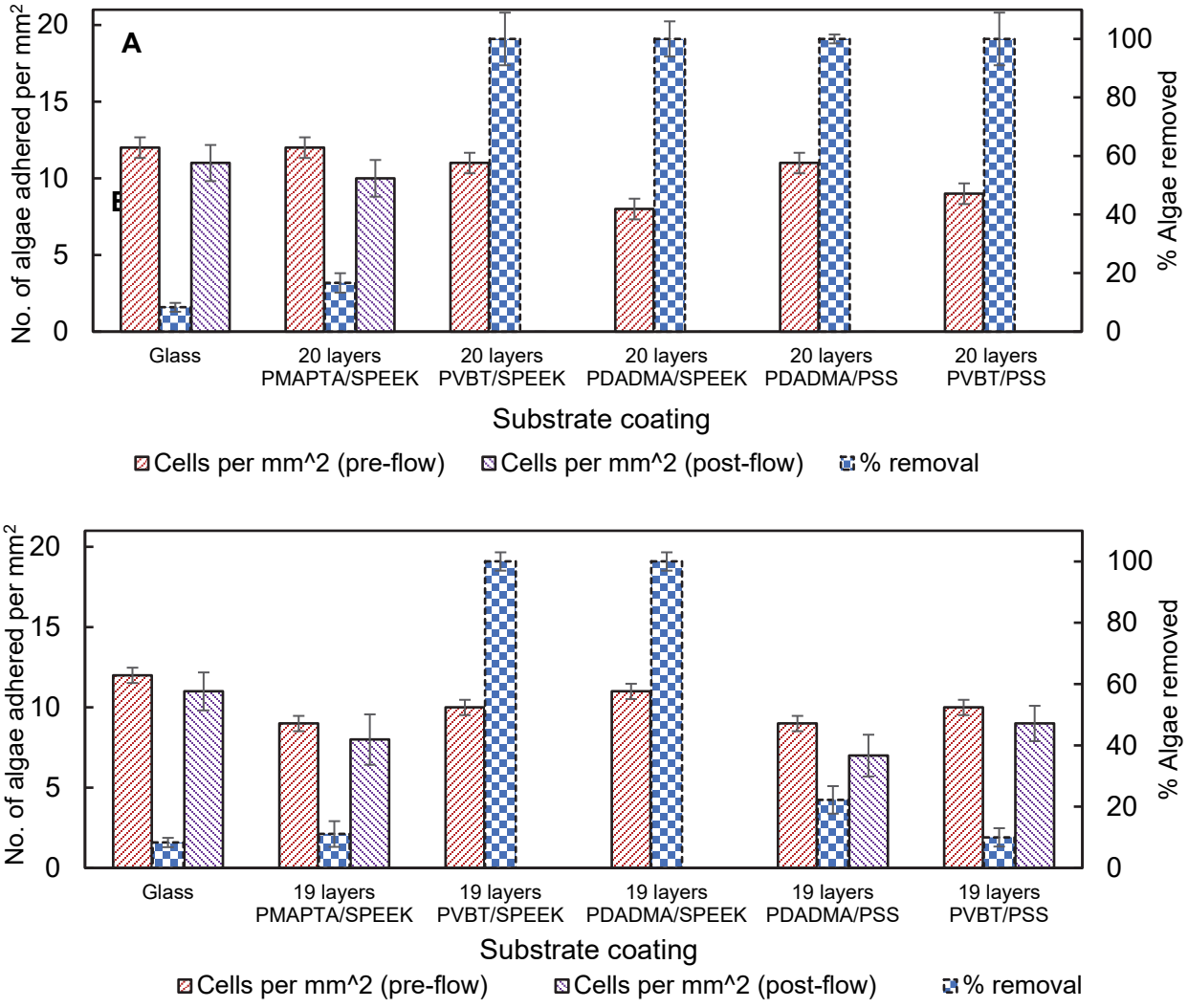

The surface charge is determined by the identity of the last layer (Figure 2), which is positive for an odd number of layers and negative for an even number (deposition always starts with the polycation). The influence of surface charge on adhesion is illustrated in Figure 7. All coatings except PMAPTA/SPEEK were effective for 20 layers, whereas two of the coatings failed to prevent algal adhesion when the number of layers was reduced to 19. The effectiveness of 19 layers of PVBT/SPEEK and PDADMA/SPEEK was surprising, but it may indicate a near-neutral surface charge. In fact, the zeta potentials for the odd PDADMA/SPEEK films were lower in magnitude than those for the even layers (Figure 2). The 20-layer PMAPTA/SPEEK film showed partial foul-release behavior over time under flow (Supporting Information Figure S15) as did the 19-layer PDADMA/PSS film (Supporting Information Figure S16).

C. reinhardtii, like many other flagellar systems, are able to interact with (interrogate) surfaces via their flagella. A negatively charged surface would electrostatically repel[64] the negatively charged N-glycan proteins that populate the cell walls of the flagella.[73] The persistent fouling seen in most of the positively-charged surfaces could be explained in a similar way. A maximum of 20% detachment of adhered algae was observed at the highest flow rate for those films. Prior studies of algae adhesion to charged surfaces revealed that positively charged surfaces enhance the adhesion of foulants such as algae[74,75] in agreement with most of the data in Figure 7B.

Conclusions

Ultrathin coatings of glassy polyelectrolyte complex were shown to be highly effective at preventing fouling by the common algae *C. reinhardtii*. Glassy coatings are not known to be antifouling, but in the present case, a water content and balanced positive and negative charges presented a surface with little driving force for adsorption. Dip- or spray-buildup of these films may be accomplished over a wide area on a variety of substrates. Viscoelastic measurements revealed no evidence for transitions in property (elastic modulus > 10 MPa) below 70 ^{o}C, suggesting the coating will remain rugged at most use temperatures. As with all antifouling coatings, performance over an extended period of time is desired and evaluations of this property are underway. Also underway are efforts to evaluate antifouling properties of these “zwitterglass” coatings using more classes of organisms, such as marine bacteria, seagrass, diatoms, and barnacles. The coatings described here pave the way towards new, more resilient, practical coatings for reducing or eliminating biofouling.

Supporting Information

Flow setup for streaming potential measurements; NMR of SPEEKLi; FTIR spectra of PEEK and SPEEK; comparison of layer-by-layer buildup of PVBT/PSS using UV-vis absorbance and ellipsometry; isothermal calorimetry titration of SPEEK with polycations; FTIR of individual polyelectrolytes and PECs; layer-by-layer assembly of PDADMA/SPEEK showing thickness increment for each layer; dynamic light scattering for SPEEKLi solutions; sectional analysis of AFM images; contact angle measurements on various SPEEK/polycation surfaces; SEM images

of SPEEK multilayers as-made and after immersion in 3 M NaCl for a week, flow setup for algae adhesion; images of algae on PDADMA/PSS before and after flow; removal of adhered algae versus flow rate on PDADMA/PAA; removal of adhered algae versus flow rate on 20 layers PMAPTA/SPEEK; removal of adhered algae versus flow rate on 19 layers PDADMA/PSS.

Corresponding Author

Joseph B. Schlenoff - Department of Chemistry and Biochemistry, The Florida State University, Tallahassee, FL 32306 USA. 0000-0001-5588-1253 Email: jschlenoff@fsu.edu

Authors

John Akintola - Department of Chemistry and Biochemistry, The Florida State University, Tallahassee, FL 32306

Yuhui Chen - Department of Chemistry and Biochemistry, The Florida State University, Tallahassee, FL 32306

Zachary A. Digby - Department of Chemistry and Biochemistry, The Florida State University, Tallahassee, FL 32306. 0000-0001-5018-9620

Notes

The authors declare no competing financial interests.

Acknowledgements

This work was supported by grants from the Office of Naval Research, N00014-23-1-2125, and the National Science Foundation, DMR 2103703.

References

1. Callow, J. A.; Callow, M. E. Trends in the Development of Environmentally Friendly Fouling-Resistant Marine Coatings. *Nat Commun* **2011,** *2*, 244.

2. Schultz, M. P.; Bendick, J. A.; Holm, E. R.; Hertel, W. M. Economic Impact of Biofouling on a Naval Surface Ship. *Biofouling* **2011,** *27*, 87-98.

3. Meloni, M.; Correa, N.; Pitombo, F. B.; Chiesa, I. L.; Doti, B.; Elías, R.; Genzano, G.; Giachetti, C. B.; Giménez, D.; López-Gappa, J.; Pastor, C.; Wandeness, A. P.; Ramírez, F. C.; Roccatagliata, D.; Schulze-Sylvester, M.; Tatián, M.; Zelaya, D. G.; Sylvester, F. In-Water and Dry-Dock Hull Fouling Assessments Reveal High Risk for Regional Translocation of Nonindigenous Species in the Southwestern Atlantic. *Hydrobiologia* **2021,** *848*, 1981-1996.

4. Chambers, L. D.; Stokes, K. R.; Walsh, F. C.; Wood, R. J. K. Modern Approaches to Marine Antifouling Coatings. *Surf Coat Tech* **2006,** *201*, 3642-3652.

5. Paz-Villarraga, C. A.; Castro, Í. B.; Fillmann, G. Biocides in Antifouling Paint Formulations Currently Registered for Use. *Environmental Science and Pollution Research* **2022,** *29*, 30090-30101.
6. Beans, C. News Feature: How "Forever Chemicals" Might Impair the Immune System. *P Natl Acad Sci USA* **2021,** *118*, e2105018118.
7. Lagerström, M.; Wrange, A.-L.; Oliveira, D. R.; Granhag, L.; Larsson, A. I.; Ytreberg, E. Are Silicone Foul-Release Coatings a Viable and Environmentally Sustainable Alternative to Biocidal Antifouling Coatings in the Baltic Sea Region? *Marine Pollution Bulletin* **2022,** *184*, 114102.
8. Ikada, Y. Blood-Compatible Polymers. *Advances in Polymer Science* **1984,** *57*, 103-140.
9. Chen, S. F.; Li, L. Y.; Zhao, C.; Zheng, J. Surface Hydration: Principles and Applications toward Low-Fouling/Nonfouling Biomaterials. *Polymer* **2010,** *51*, 5283-5293.
10. Luk, Y. Y.; Kato, M.; Mrksich, M. Self-Assembled Monolayers of Alkanethiolates Presenting Mannitol Groups Are Inert to Protein Adsorption and Cell Attachment. *Langmuir* **2000,** *16*, 9604-9608.
11. Jeon, S. I.; Lee, J. H.; Andrade, J. D.; Degennes, P. G. Protein Surface Interactions in the Presence of Polyethylene Oxide .1. Simplified Theory. *J Colloid Interf Sci* **1991,** *142*, 149-158.
12. Currie, E. P. K.; Norde, W.; Cohen Stuart, M. A. Tethered Polymer Chains: Surface Chemistry and Their Impact on Colloidal and Surface Properties. *Adv Colloid Interfac* **2003,** *100–102*, 205-265.
13. Milatz, R.; Duvigneau, J.; Vancso, G. J. Dopamine-Based Copolymer Bottlebrushes for Functional Adhesives: Synthesis, Characterization, and Applications in Surface Engineering of Antifouling Polyethylene. *ACS Applied Materials & Interfaces* **2023**, 15, 34023–34030.
14. Sarker, P.; Lu, T.; Liu, D.; Wu, G.; Chen, H.; Jahan Sajib, M. S.; Jiang, S.; Chen, Z.; Wei, T. Hydration Behaviors of Nonfouling Zwitterionic Materials. *Chemical Science* **2023**, 14, 7500-7511.
15. Ostuni, E.; Chapman, R. G.; Liang, M. N.; Meluleni, G.; Pier, G.; Ingber, D. E.; Whitesides, G. M. Self-Assembled Monolayers That Resist the Adsorption of Proteins and the Adhesion of Bacterial and Mammalian Cells. *Langmuir* **2001,** *17*, 6336-6343.
16. Zou, P.; Hartleb, W.; Lienkamp, K. It Takes Walls and Knights to Defend a Castle - Synthesis of Surface Coatings from Antimicrobial and Antibiofouling Polymers. *J Mater Chem* **2012,** *22*, 19579-19589.
17. Chiang, C.-T.; Vu, V. T.; Cheng, Y.-T.; Huang, C.-J. Methacrylate Silatrane: New Building Block for Development of Functional Polymeric Coatings through Controlled Silanization. *ACS Applied Materials & Interfaces* **2023,** *15*, 28524-28535.
18. Chen, X. Y.; Armes, S. P. Surface Polymerization of Hydrophilic Methacrylates from Ultrafine Silica Sols in Protic Media at Ambient Temperature: A Novel Approach to Surface Functionalization Using a Polyelectrolytic Macroinitiator. *Advanced Materials* **2003,** *15*, 1558-1562.
19. Terayama, Y.; Kikuchi, M.; Kobayashi, M.; Takahara, A. Well-Defined Poly(Sulfobetaine) Brushes Prepared by Surface-Initiated ATRP Using a Fluoroalcohol and Ionic Liquids as the Solvents. *Macromolecules* **2011,** *44*, 104-111.
20. Jiang, W.; Irgum, K. Tentacle-Type Zwitterionic Stationary Phase, Prepared by Surface-Initiated Graft Polymerization of 3-[N,N-Dimethyl-N-(Methacryloyloxyethyl)-Ammonium] Propanesulfonate through Peroxide Groups Tethered on Porous Silica. *Anal Chem* **2002,** *74*, 4682-4687.
21. Zhang, Z.; Chen, S.; Chang, Y.; Jiang, S. Surface Grafted Sulfobetaine Polymers Via Atom Transfer Radical Polymerization as Superlow Fouling Coatings. *The Journal of Physical Chemistry B* **2006,** *110*, 10799-10804.

22. Zhang, Z.; Finlay, J. A.; Wang, L. F.; Gao, Y.; Callow, J. A.; Callow, M. E.; Jiang, S. Y. Polysulfobetaine-Grafted Surfaces as Environmentally Benign Ultralow Fouling Marine Coatings. *Langmuir* **2009,** *25*, 13516-13521.
23. Cheng, G.; Zhang, Z.; Chen, S. F.; Bryers, J. D.; Jiang, S. Y. Inhibition of Bacterial Adhesion and Biofilm Formation on Zwitterionic Surfaces. *Biomaterials* **2007,** *28*, 4192-4199.
24. Jiang, C.; Wang, G.; Hein, R.; Liu, N.; Luo, X.; Davis, J. J. Antifouling Strategies for Selective in Vitro and in Vivo Sensing. *Chemical Reviews* **2020,** *120*, 3852-3889.
25. Tugulu, S.; Klok, H.-A. Stability and Nonfouling Properties of Poly(Poly(Ethylene Glycol) Methacrylate) Brushes under Cell Culture Conditions. *Biomacromolecules* **2008,** *9*, 906-912.
26. Chen, W.-L.; Menzel, M.; Watanabe, T.; Prucker, O.; Rühe, J.; Ober, C. K. Reduced Lateral Confinement and Its Effect on Stability in Patterned Strong Polyelectrolyte Brushes. *Langmuir* **2017,** *33*, 3296-3303.
27. Ding, Z.; Chen, C.; Yu, Y.; de Beer, S. Synthetic Strategies to Enhance the Long-Term Stability of Polymer Brush Coatings. *J Mater Chem B* **2022,** *10*, 2430-2443.
28. Fu, J. C.; Schlenoff, J. B. Driving Forces for Oppositely Charged Polyion Association in Aqueous Solutions: Enthalpic, Entropic, but Not Electrostatic. *Journal of the American Chemical Society* **2016,** *138*, 980-990.
29. Kitano, H.; Imai, M.; Sudo, K.; Ide, M. Hydrogen-Bonded Network Structure of Water in Aqueous Solution of Sulfobetaine Polymers. *Journal of Physical Chemistry B* **2002,** *106*, 11391-11396.
30. Schlenoff, J. B. Zwitteration: Coating Surfaces with Zwitterionic Functionality to Reduce Nonspecific Adsorption. *Langmuir* **2014,** *30*, 9625-9636.
31. Chen, Y.; Yang, M.; Schlenoff, J. B. Glass Transitions in Hydrated Polyelectrolyte Complexes. *Macromolecules* **2021,** *54*, 3822-3831.
32. Ghostine, R. A.; Markarian, M. Z.; Schlenoff, J. B. Asymmetric Growth in Polyelectrolyte Multilayers. *Journal of the American Chemical Society* **2013,** *135*, 7636-7646.
33. Huang, H.; Zhang, C.; Crisci, R.; Lu, T.; Hung, H.-C.; Sajib, M. S. J.; Sarker, P.; Ma, J.; Wei, T.; Jiang, S.; Chen, Z. Strong Surface Hydration and Salt Resistant Mechanism of a New Nonfouling Zwitterionic Polymer Based on Protein Stabilizer TMAO. *Journal of the American Chemical Society* **2021,** *143*, 16786-16795.
34. Graul, T. W.; Schlenoff, J. B. Capillaries Modified by Polyelectrolyte Multilayers for Electrophoretic Separations. *Analytical Chemistry* **1999,** *71*, 4007-4013.
35. Salloum, D. S.; Olenych, S. G.; Keller, T. C. S.; Schlenoff, J. B. Vascular Smooth Muscle Cells on Polyelectrolyte Multilayers: Hydrophobicity-Directed Adhesion and Growth. *Biomacromolecules* **2005,** *6*, 161-167.
36. Arias, C. J.; Keller, T. C. S.; Schlenoff, J. B. Quasi-Spherical Cell Clusters Induced by a Polyelectrolyte Multilayer. *Langmuir* **2015,** *31*, 6436-6446.
37. Ghoussoub, Y. E.; Fares, H. M.; Delgado, J. D.; Keller, L. R.; Schlenoff, J. B. Antifouling Ion-Exchange Resins. *ACS Applied Materials and Interfaces* **2018,** *10*, 41747-41756.
38. Müller, M.; Rieser, T.; Lunkwitz, K.; Meier-Haack, J. Polyelectrolyte Complex Layers: A Promising Concept for Antifouling Coatings Verified by in-Situ ATR-FTIR Spectroscopy. *Macromolecular Rapid Communications* **1999,** *20*, 607-611.

39. Thierry, B.; Winnik, F. M.; Merhi, Y.; Silver, J.; Tabrizian, M. Bioactive Coatings of Endovascular Stents Based on Polyelectrolyte Multilayers. *Biomacromolecules* **2003,** *4*, 1564-1571.
40. Mendelsohn, J. D.; Yang, S. Y.; Hiller, J.; Hochbaum, A. I.; Rubner, M. F. Rational Design of Cytophilic and Cytophobic Polyelectrolyte Multilayer Thin Films. *Biomacromolecules* **2003,** *4*, 96-106.
41. Sendra, M.; Yeste, M. P.; Gatica, J. M.; Moreno-Garrido, I.; Blasco, J. Direct and Indirect Effects of Silver Nanoparticles on Freshwater and Marine Microalgae (Chlamydomonas Reinhardtii and Phaeodactylum Tricornutum). *Chemosphere* **2017,** *179*, 279-289.
42. Tesler, A. B.; Kim, P.; Kolle, S.; Howell, C.; Ahanotu, O.; Aizenberg, J. Extremely Durable Biofouling-Resistant Metallic Surfaces Based on Electrodeposited Nanoporous Tungstite Films on Steel. *Nat. Commun.* **2015,** *6*, 8649.
43. Kooten, T. G. V. S., M.; Busscher, H. J. Development and Use of a Parallel-Plate Flow Chamber for Studying Cellular Adhesion to Solid Surfaces. *J. Biomed. Mater. Res.* **1992,** *26*, 725-738.
44. Sager, R., and Granick, S. Nutritional Studies with Chlamydomonas Reinhardi. *Ann. N. Y. Acad. Sci.* **1953,** *56*, 831-838.
45. Decher, G. Fuzzy Nanoassemblies: Toward Layered Polymeric Multicomposites. *Science* **1997,** *277*, 1232-1237.
46. Shibuya, N. P., R. S. A Kinetic Study of PEEK Sulfonation in Concentrated Sulfuric Acid by Ultraviolet Visible Spectroscopy. *Polymer* **1994,** *35*, 3237-3242.
47. Gu, Y.; Li, D. The Zeta-Potential of Glass Surface in Contact with Aqueous Solutions. *Journal of Colloid and Interface Science* **2000,** *226*, 328-339.
48. Montero, J. F.; Tajiri, H. A.; Barra, G. M.; Fredel, M. C.; Benfatti, C. A.; Magini, R. S.; Pimenta, A. L.; Souza, J. C. Biofilm Behavior on Sulfonated Poly(Ether-Ether-Ketone) (SPEEK). *Mater. Sci. Eng. C.* **2017,** *70*, 456-460.
49. Hariri, H. H.; Lehaf, A. M.; Schlenoff, J. B. Mechanical Properties of Osmotically Stressed Polyelectrolyte Complexes and Multilayers: Water as a Plasticizer. *Macromolecules* **2012,** *45*, 9364-9372.
50. Batys, P.; Zhang, Y.; Lutkenhaus, J. L.; Sammalkorpi, M. Hydration and Temperature Response of Water Mobility in Poly(Diallyldimethylammonium)–Poly(Sodium 4-Styrenesulfonate) Complexes. *Macromolecules* **2018,** *51*, 8268-8277.
51. Dubas, S. T.; Farhat, T. R.; Schlenoff, J. B. Multiple Membranes from "True" Polyelectrolyte Multilayers. *Journal of the American Chemical Society* **2001,** *123*, 5368-5369.
52. Schlenoff, J. B.; Dubas, S. T.; Farhat, T. Sprayed Polyelectrolyte Multilayers. *Langmuir* **2000,** *16*, 9968-9969.
53. Kurtz, I. S.; Sui, S.; Hao, X.; Huang, M.; Perry, S. L.; Schiffman, J. D. Bacteria-Resistant, Transparent, Free-Standing Films Prepared from Complex Coacervates. *ACS Applied Bio Materials* **2019,** *2*, 3926-3933.
54. Zhu, X.; Jańczewski, D.; Lee, S. S. C.; Teo, S. L.-M.; Vancso, G. J. Cross-Linked Polyelectrolyte Multilayers for Marine Antifouling Applications. *ACS Applied Materials & Interfaces* **2013,** *5*, 5961-5968.
55. Picart, C.; Mutterer, J.; Richert, L.; Luo, Y.; Prestwich, G. D.; Schaaf, P.; Voegel, J. C.; Lavalle, P. Molecular Basis for the Explanation of the Exponential Growth of Polyelectrolyte Multilayers. *Proceedings of the National Academy of Sciences of the United States of America* **2002,** *99*, 12531-12535.
56. Laugel, N.; Betscha, C.; Winterhalter, M.; Voegel, J. C.; Schaaf, P.; Ball, V. Relationship between the Growth Regime of Polyelectrolyte Multilayers and the Polyanion/Polycation Complexation Enthalpy. *Journal of Physical Chemistry B* **2006,** *110*, 19443-19449.

57. Porcel, C.; Lavalle, P.; Ball, V.; Decher, G.; Senger, B.; Voegel, J. C.; Schaaf, P. From Exponential to Linear Growth in Polyelectrolyte Multilayers. *Langmuir* **2006,** *22*, 4376-4383.
58. Xing, P.; Robertson, G. P.; Guiver, M. D.; Mikhailenko, S. D.; Wang, K.; Kaliaguine, S. Synthesis and Characterization of Sulfonated Poly(Ether Ether Ketone) for Proton Exchange Membranes. *Journal of Membrane Science* **2004,** *229*, 95-106.
59. Priftis, D.; Laugel, N.; Tirrell, M. Thermodynamic Characterization of Polypeptide Complex Coacervation. *Langmuir* **2012,** *28*, 15947-15957.
60. Liu, C.; Lee, J.; Ma, J.; Elimelech, M. Antifouling Thin-Film Composite Membranes by Controlled Architecture of Zwitterionic Polymer Brush Layer. *Environmental Science & Technology* **2017,** *51*, 2161-2169.
61. Feng, Z.; Feng, X.; Lu, X. Bioinspired N-Oxide-Based Zwitterionic Polymer Brushes for Robust Fouling-Resistant Surfaces. *Environmental Science & Technology* **2023,** *57*, 7298-7308.
62. Beyer, C. D.; Thavalingam, S.; Guseva, T.; Schardt, L.; Zimmermann, R.; Werner, C.; Dietze, P.; Bandow, J. E.; Metzler-Nolte, N.; Rosenhahn, A. Zwitterionic Peptides Reduce Accumulation of Marine and Freshwater Biofilm Formers. *ACS Applied Materials & Interfaces* **2021,** *13*, 49682-49691.
63. Hunter, R. J. *Introduction to Modern Colloid Science, Ch. 7 & 8*; Oxford University Press: Oxford, 1993. p 338.
64. Howell, D.; Behrends, B. A Review of Surface Roughness in Antifouling Coatings Illustrating the Importance of Cutoff Length. *Biofouling* **2006,** *22*, 401-410.
65. Ciriminna, R.; Bright, F. V.; Pagliaro, M. Ecofriendly Antifouling Marine Coatings. *ACS Sustain Chem Eng* **2015,** *3*, 559-565.
66. Petronis, Š.; Berntsson, K.; Gold, J.; Gatenholm, P. Design and Microstructuring of Pdms Surfaces for Improved Marine Biofouling Resistance. *Journal of Biomaterials Science, Polymer Edition* **2000,** *11*, 1051-1072.
67. Schumacher, J. F.; Carman, M. L.; Estes, T. G.; Feinberg, A. W.; Wilson, L. H.; Callow, M. E.; Callow, J. A.; Finlay, J. A.; Brennan, A. B. Engineered Antifouling Microtopographies - Effect of Feature Size, Geometry, and Roughness on Settlement of Zoospores of the Green Alga Ulva. *Biofouling* **2007,** *23*, 55-62.
68. Scardino, A. J.; Harvey, E.; De Nys, R. Testing Attachment Point Theory: Diatom Attachment on Microtextured Polyimide Biomimics. *Biofouling* **2006,** *22*, 55-60.
69. Cui, Y.; Yuan, W. Q.; Cao, J. Effects of Surface Texturing on Microalgal Cell Attachment to Solid Carriers. *Int. J. Agric. & Biol. Eng* **2013,** *6*, 44-54.
70. Dubas, S. T.; Schlenoff, J. B. Polyelectrolyte Multilayers Containing a Weak Polyacid: Construction and Deconstruction. *Macromolecules* **2001,** *34*, 3736-3740.
71. Dautzenberg, H.; Kriz, J. Response of Polyelectrolyte Complexes to Subsequent Addition of Salts with Different Cations. *Langmuir* **2003,** *19*, 5204-5211.
72. Perry, S. L.; Li, Y.; Priftis, D.; Leon, L.; Tirrell, M. The Effect of Salt on the Complex Coacervation of Vinyl Polyelectrolytes. *Polymers* **2014,** *6*, 1756-1772.
73. Xu, N.; Oltmanns, A.; Zhao, L.; Girot, A.; Karimi, M.; Hoepfner, L.; Kelterborn, S.; Scholz, M.; Beißel, J.; Hegemann, P.; Bäumchen, O.; Liu, L.-N.; Huang, K.; Hippler, M. Altered N-Glycan Composition Impacts Flagella-Mediated Adhesion in Chlamydomonas Reinhardtii. *eLife* **2020,** *9*, e58805.

74. Ederth, T.; Nygren, P.; Pettitt, M. E.; Ostblom, M.; Du, C.; Broo, K.; Callow, M. E.; Callow, J.; Liedberg, B. Anomalous Settlement Behavior of Ulva Linza Zoospores on Cationic Oligopeptide Surfaces. *Biofouling* **2008,** *24*, 303-12.
75. Ge, S.; Agbakpe, M.; Zhang, W.; Kuang, L. Heteroaggregation between PEI-Coated Magnetic Nanoparticles and Algae: Effect of Particle Size on Algal Harvesting Efficiency. *ACS Appl. Mater. Interfaces* **2015,** *7*, 6102-8.